JOURNAL OF MATERIALS SCIENCE 22 (1987) 4453–4459

Effect of silane coupling agent on vulcanization, network structure, polymer–filler interaction, physical properties and failure mode of mica-filled styrene–butadiene rubber

S. DEBNATH, S. K. DE, D. KHASTGIR
Rubber Technology Centre, Indian Institute of Technology, Kharagpur 721 302, India

Physical properties of composites from mica and styrene–butadiene rubber (SBR) have been studied with special reference to the effect of silane coupling agent (A-174) in the compound. Tensile and tear properties increase with the addition of mica. The increase of tensile properties is more pronounced in the case of silane-treated mica. Silane treatment also raises the volume fraction of rubber in solvent-swollen rubber vulcanizate. Attempts have been made to correlate the changes in properties with the network structure of rubber. In order to understand the mechanism of failure, tensile fracture surfaces have been examined by scanning electron microscopy (SEM). The fractographs have been correlated with the strength and type of failure of these composites. The observed values of viscosity (rheometric) correspond to the calculated values from existing theory based on the hydrodynamic model of dispersed particles in a fluid medium.

1. Introduction

Mica has been used as a filler for thermoplastics due to its low cost, easy availability and outstanding electrical, heat and chemical resistance. The extent of reinforcement by mica depends on the aspect ratio (that is, ratio of length to thickness). The effects of high aspect ratio mica on the mechanical properties of thermosets and thermoplastics have been studied [1, 2]. Breakdown of mica particles during mixing and processing causes reduction of aspect ratio [3]. The use of hot runners, longer sprues and streamlining reduce particle breakdown [4].

Rheological properties [5–7] of mica-filled polyolefins have been extensively studied. Schreiber *et al.* [5, 8, 9] have described the flow, mechanical and electrical properties of plasma-treated mica. The enhancement of mica–polymer interaction by treatment of mica by titania [10], chlorinated paraffin [11] and silane coupling agent [12, 13] has been studied earlier. Tausz and Chaffey [4] compared the mechanical properties of ultrasonically delaminated mica with those of conventional mica in poly(propylene) matrix. However, reports on the use of mica as filler in rubber are scant. It has been reported that mica-enhanced anisometric swelling of nitrile rubber vulcanizate [15] and reduces permeability of gases [16].

The present paper deals with the effects of muscovite 3 μm mica on vulcanization, network structure, physical properties and failure of styrene–butadiene rubber (SBR). SBR was chosen because it is non strain-crystallizing and the reinforcing effect of mica can be easily manifested in such a system.

A silane coupling agent (gamma-methacryloxy propyl trimethoxy silane, A-174) was used to study its effect on sulphur vulcanization, network structure, polymer–filler interaction, physical properties and failure mode of mica–rubber composites.

2. Experimental details

2.1. Materials used

SBR-1502, a styrene–butadiene copolymer rubber, containing 23% styrene, manufactured by Synthetics and Chemicals, Bareily, India, was used in the present studies. Muscovite mica (3 μm) used for this study was supplied by Mica Trading Corporation of India, Patna. Accelerators, *N*-cyclohexyl-2-benzothiazyl sulphenamide (CBS) and zinc dithiocarbamate (ZDC) were obtained from IEL Ltd, Rishra, India, and the silane coupling agent (A-174) was supplied by Union Carbide UK Ltd. Other compounding ingredients such as zinc oxide, stearic acid, sulphur and the solvent benzene were of commercial grade.

2.2. Preparation of mixes, rheometry and preparation of test samples

Formulations of the mixes are given in Table I. Mixing was done on an open two-rolls mill with a nip gap of 0.25 mm and at a friction ratio of 1 : 1.10 at 70° C.

Optimum cure time at 150° C was obtained from the rheographs (Figs 1 and 2) obtained from Monsanto Rheometer R-100. Vulcanization of mixes was done in an electrically heated press at 150° C and at a pressure of 0.34 MPa. Mouldings were cooled rapidly in water at the end of the curing cycles and then conditioned

0022–2461/87 $03.00 + .12

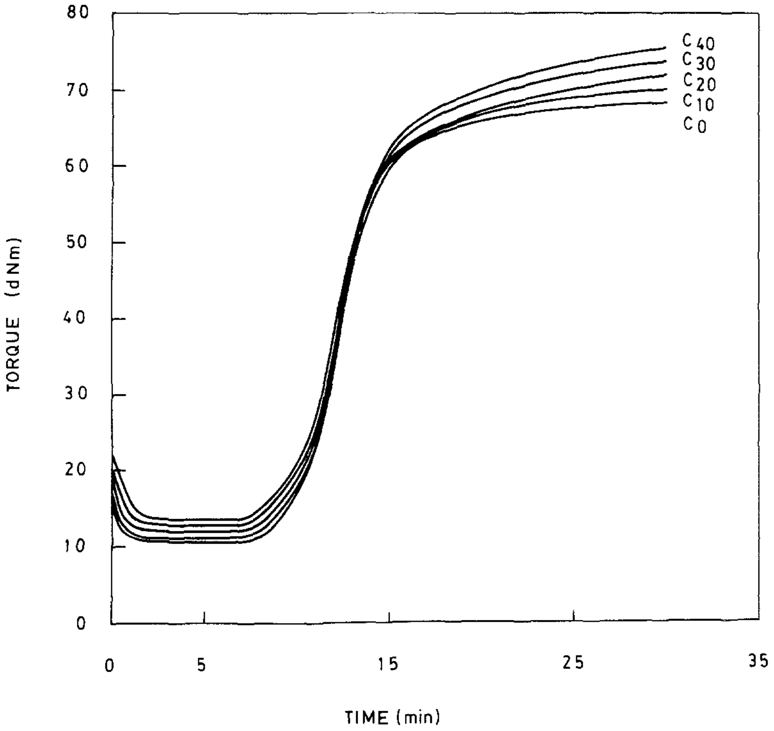

Figure 1 Rheographs of mica-filled mixes of SBR-1502 at 150° C.

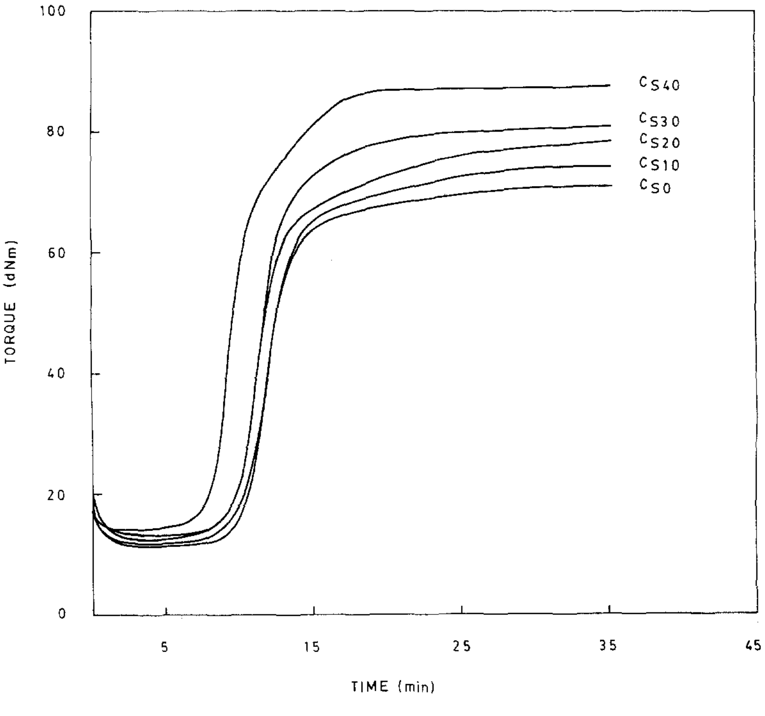

Figure 2 Rheographs of silane (A-174)-treated mica-filled mixes of SBR-1502 at 150° C.

TABLE I Formulations of the mixes

	Mix no.									
	C_0	C_{10}	C_{20}	C_{30}	C_{40}	C_{S0}	C_{S10}	C_{S20}	C_{S30}	C_{S40}
SBR-1502	100	100	100	100	100	100	100	100	100	100
Zinc oxide	5	5	5	5	5	5	5	5	5	5
Stearic acid	2	2	2	2	2	2	2	2	2	2
Mica	–	10	20	30	40	–	10	20	30	40
A-174	–	–	–	–	–	1	1	2	3	4
CBS	1	1	1	1	1	1	1	1	1	1
ZDC	0.25	0.25	0.25	0.25	0.25	0.25	0.25	0.25	0.25	0.25
Sulphur	2	2	2	2	2	2	2	2	2	2

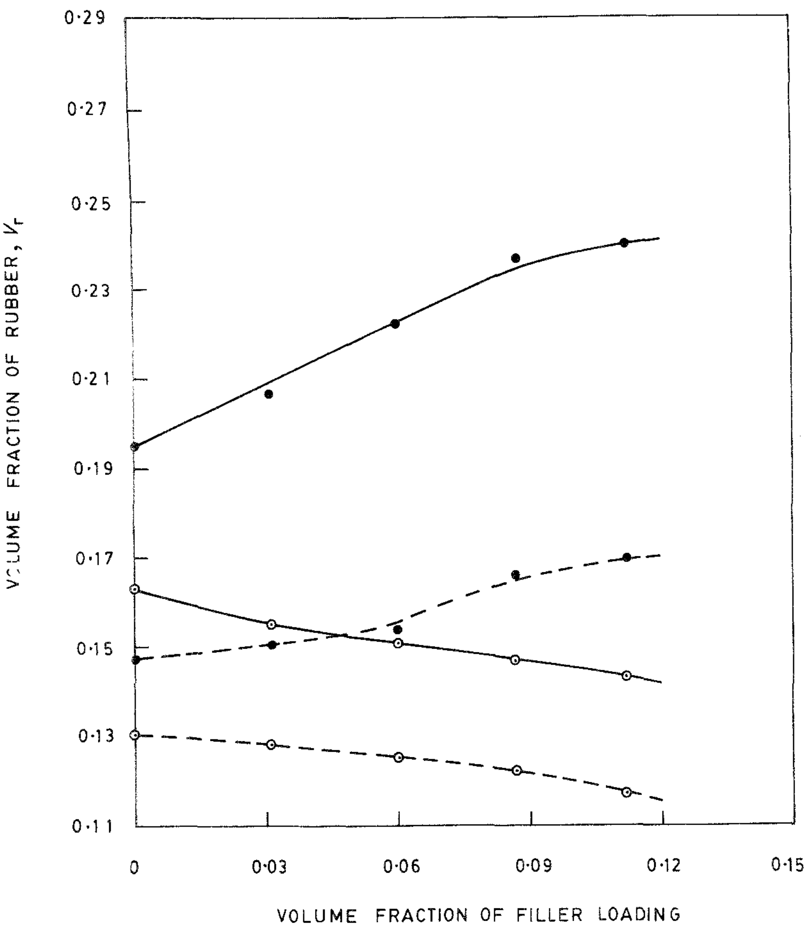

Figure 3 Plots of volume fractions of rubber as a function of filler loading. (○) Untreated mica, (●) silane (A-174)-treated mica, (——) before thiol-amine treatment, (– – –) after thiol-amine treatment.

for 24 h before testing. All properties were measured along the machine direction.

2.3. Physical testing of the samples

Stress–strain data were determined using an Instron Universal testing machine (model 1195) using ASTM C type dumb-bell specimen according to ASTM D 412-51T. Tear strength was determined according to ASTM D 624-81 test method using 90° angle test pieces. Abrasion resistance was determined in a DuPont Cryodon abrader according to ASTM D 394, method A.

A Dunlop tripsometer was used to measure rebound resilience at 35° C according to BS 903, Pt. 22, 1950. A Goodrich flexometer was used to measure heat-build-up and dynamic set according to ASTM D 623-67, method A.

Compression set at constant stress (187 kg) and the same at constant strain (25%) were measured according to ASTM methods D 395-61, method A and D 395-61, method B, respectively.

2.4. Chemical testing of the samples

Volume fraction of rubber (V_r) in the vulcanizates was determined by an equilibrium swelling method in benzene at 37° C using the following equation [17]

$$V_r = \frac{(D - FT)\,\varrho_r^{-1}}{(D - FT)\,\varrho_r^{-1} + A_0\varrho_s^{-1}} \qquad (1)$$

where, T is the weight of the test specimen, F the weight fraction of the insoluble components in the sample, D the unswollen weight of the test specimen, A_0 the weight of absorbed solvent, corrected for swelling increment, ϱ_r the density of rubber and ϱ_s the density of solvent.

Thiol-amine treatment is believed to cause cleavage of polysulphide linkages [18]. Therefore, assuming V_r as a measure of the chemical crosslink density, the difference in V_r before and after thiol-amine treatment is believed to be a measure of the polysulphide crosslink density in the total crosslinks of the network structure.

2.5. Scanning electron microscopy studies

The SEM observations of tensile failure surfaces were made using a Philips 500 model scanning electron microscope. The failure surfaces of the test samples were carefully cut out and then sputter coated with gold within 24 h of testing. The tilt was kept at 0° in all cases.

TABLE II Curing characteristics of the mixes at 150° C using Monsanto rheometer (R-100)

	Mix no.									
	C_0	C_{10}	C_{20}	C_{30}	C_{40}	C_{S0}	C_{S10}	C_{S20}	C_{S30}	C_{S40}
Minimum torque (dN m)	10.5	11.2	12.0	12.8	13.6	11.0	11.5	12.0	12.7	13.5
Maximum torque (dN m)	67.5	70.0	71.7	73.5	75.3	72.0	74.5	78.5	81.0	85.5
Optimum cure time (min)	15.5	17.0	17.5	17.5	17.5	16.0	17.0	17.0	16.0	16.0
Cure rate ($\min^{-1}$)	9.1	8.2	8.0	7.5	7.7	8.0	8.0	8.2	9.1	10.0

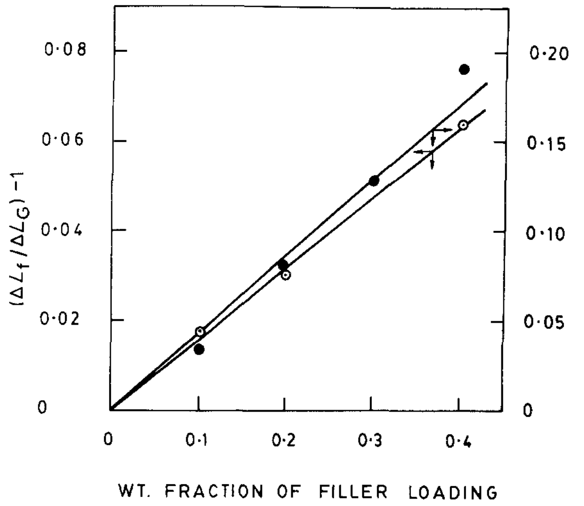

Figure 4 Plots according to Westlinning–Wolff's equation [20]. (○) Untreated mica, (●) silane (A-174)-treated mica.

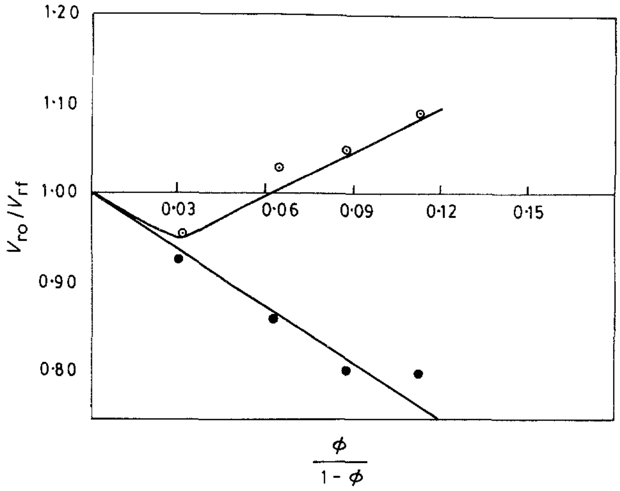

Figure 5 Plots according to Kraüs equation [21, 22]. (○) Untreated mica, (●) silane (A-174)-treated mica.

3. Results and discussion

3.1. Curing characteristics

Rheographs are shown in Figs 1 and 2. Curing characteristics are shown in Table II. Cure rate decreases on addition of mica, but it increases in the case of silane-treated mica, indicating absorption of a part of the curvatures on the filler surface which, however, decreases on silane treatment. This is also manifested in the case of optimum cure time. Untreated mica causes marginal increase in optimum cure time, but silane-treated mica does not alter the optimum cure time significantly. Moreover, silane treatment increases the rate of vulcanization as well as the maximum torque in the rheographs.

As expected mica, increases the minimum viscosity, but silane does not have any significant effect on the minimum viscosity. This indicates that silane causes no change in the plasticity of the unvulcanized rubber compound.

3.2. Network structure

Fig. 3 shows the V_r values of vulcanizates before and after thiol-amine treatment. It is evident that mica causes a decrease of V_r values. However, addition of silane-treated mica increases it. Virtually no change is observed in the polysulphidic crosslink density due to addition of mica, where a significant increase in polysulphidic crosslink density is observed when silane-treated mica is used. A lowering of crosslink density as a consequence of mica addition increases the elongation at break [19] (Table III).

3.3. Mica–Rubber interaction

Fig. 4 shows the plots according to Westlinning–Wolff's equation [20].

$$\alpha_F = \left(\frac{\Delta L_f}{\Delta L_g} - 1\right)\Big/ W \tag{2}$$

where ΔL_f and ΔL_g are the rheometric torque differences between maximum and minimum torques for filled and gum compounds; W is the weight fraction of filler to polymer; α_F, obtained from the slope of $[(\Delta L_f/\Delta L_g) - 1]$ against W plot, is known to represent the filler activity. Fig. 4 yields and α_F value of 0.15 for untreated mica and a value of 0.42 for silane-treated mica, which indicates enhanced mica–rubber interaction due to silane.

Fig. 5 shows the plot of V_{ro}/V_{rf} against $\phi/(1 - \phi)$ according to the Kraüs equation [21, 22]

$$\frac{V_{ro}}{V_{rf}} = 1 - \frac{m\phi}{1-\phi} \tag{3}$$

TABLE III Physical properties of vulcanizates

	Mix no.									
	C_0	C_{10}	C_{20}	C_{30}	C_{40}	C_{S0}	C_{S10}	C_{S20}	C_{S30}	C_{S40}
Tensile strength (MPa)	2.20	2.95	3.65	3.70	3.75	2.37	3.10	3.70	4.80	5.80
100% modulus (MPa)	1.20	1.40	1.60	1.70	1.70	1.30	1.60	1.70	2.10	2.50
300% modulus (MPa)	–	2.15	2.40	2.40	2.45	–	2.90	2.80	3.50	3.90
Elongation at break (%)	290	380	410	390	380	250	305	365	365	395
Tear strength ($kN\,m^{-1}$)	12.4	13.7	15.1	21.1	19.9	11.5	14.8	15.1	18.5	17.0
Hardness (IRHD)	44.0	50.0	54.5	55.5	59.5	43.5	49.0	53.5	55.0	59.0
Density ($g\,cm^{-3}$)	0.98	1.08	1.12	1.16	1.20	1.00	1.08	1.12	1.16	1.21
Abrasion loss ($cm^3\,h^{-1}$)	0.95	1.40	1.85	1.85	1.80	0.55	0.70	1.50	1.50	1.60
Resilience (%)	61.5	67.0	69.0	67.0	66.5	64.0	62.0	60.0	59.0	56.0
Heat build-up (°C)	9.0	10.0	10.0	13.0	14.0	11.0	17.0	21.0	23.0	23.0
Dynamic set (%)	0.6	2.1	0.9	1.1	1.2	0.7	0.9	1.4	1.4	1.8
Compression set at constant strain (%)	14.6	24.3	28.7	42.0	41.7	23.6	24.7	26.4	27.1	31.2
Compression set at constant stress (%)	2.8	6.2	8.2	10.0	11.2	5.6	3.9	4.0	4.0	6.0

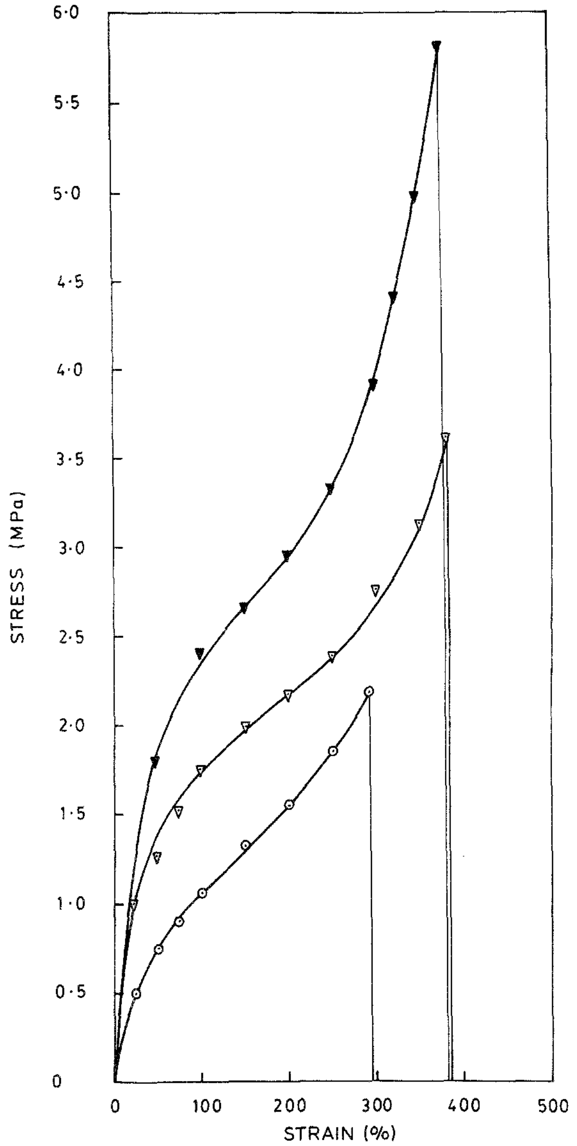

Figure 6 Stress–strain curves of gum, silane (A-174)-treated and untreated mica-filled styrene–butadiene rubber vulcanizates. (○) C_0, (▽) C_{40}, (▼) C_{S40}.

where

$$m = 3C(1 - V_{ro}^{1/3}) + V_{ro} - 1 \qquad (4)$$

and where C is a constant characteristic of filler, but independent of solvent. V_{ro} and V_{rf} are the volume fractions of rubber for gum and filled compound, ϕ is the volume fraction of filler in the vulcanizates, m is the "polymer–filler interaction" parameter obtained from the slope of the plot of V_{ro}/V_{rf} against $\phi/1 - \phi$. C can be obtained from the plot of $(m - V_{ro})$ against $(1 - V_{ro}^{1/3})$. Fig. 5 and Equation 4 yield values of m and C of 1.93 and 2.15, respectively, for silane-treated mica. Untreated mica shows non-reinforcing characteristics beyond 10 p.h.r. and therefore m has no significance in this case. However, silane-treated mica shows reinforcing characteristics at all filler loadings studied.

3.4. Physical properties

Physical properties are summarized in Table III. Mica causes marginal improvement in modulus and tensile strength. However, the increase is more pronounced in the presence of a silane coupling agent. This may be ascribed to enhanced polymer–filler interaction in the case of silane-treated mica, which is also manifested in the hysteresis values. For example, heat build-up increases in the presence of mica, but the increase is more pronounced in the case of treated mica. Similarly, resilience, as well as dynamic set, are lower in the case of silane-treated mica. Elongation at break increases in the presence of mica due to a decrease in the crosslink density [19], as measured by V_r values.

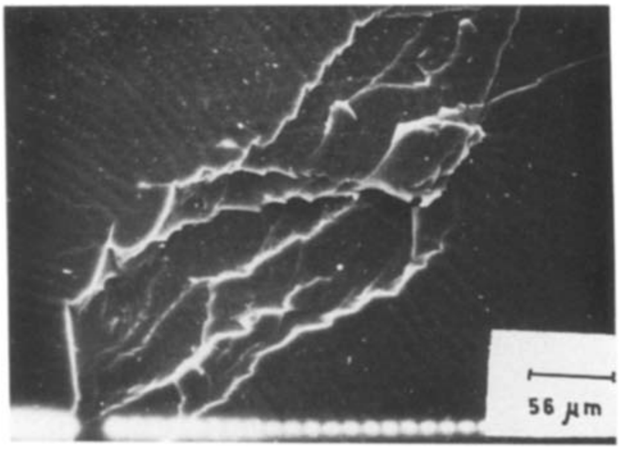

Figure 7 Scanning electron micrograph of the tensile fracture surface of mix C_0, showing brittle-type failure.

Abrasion loss in mica-filled rubber vulcanizate is less in presence of silane because of enhanced mica–polymer interaction. Mica causes a moderate increase in tear resistance. However, silane has no effect on tear resistance. As expected, compression set values increase on addition of mica, but silane causes an improvement of set properties. For example, compression set at constant stress of 20 p.h.r. mica-loaded SBR vulcanizate decreases from 8.2% to 4.0% in presence of silane.

3.5. Stress–strain properties

The stress–strain behaviour of untreated and silane-treated mica filled SBR vulcanizates are shown in Fig. 6.

Addition of mica does not make the vulcanizate rigid, as is evident from the higher percentage of elongation at break at high mica loading. Silane-treated mica raises the modulus more than the untreated mica and initial slopes becomes steeper at higher mica loading. The higher modulus of silane-treated mica is due to higher crosslink density than the untreated mica filled vulcanizates. In the case of vulcanizates loaded with 20, 30 and 40 p.h.r. mica, the sharp rise of stress indicates the orientation of mica along the direction of applied force [23]. This is also evident from the scanning electron micrograph (Fig. 8), discussed later in this paper.

The tensile fractograph of gum SBR vulcanizate (Fig. 7) shows brittle fracture. The failure pattern changes in the presence of mica (Fig. 8). The orientation of mica particles along the machine direction is also evident. Fig. 9 shows the tensile fractograph of silane-treated mica–SBR composite. The improved adhesion between mica and rubber is apparent. The results are in conformity with our observations of the

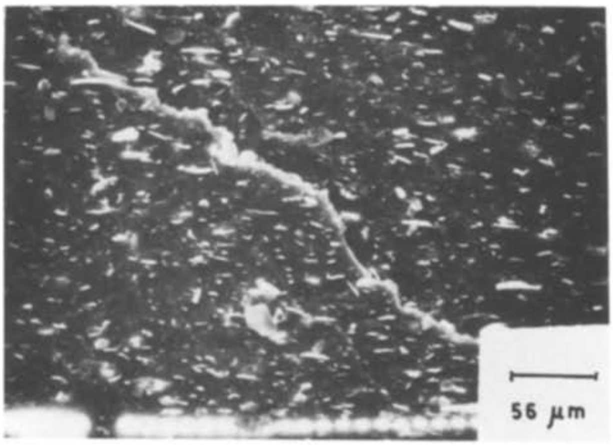

Figure 8 Scanning electron micrograph of the tensile fracture surface of mix C_{20X}, showing ductile-type failure.

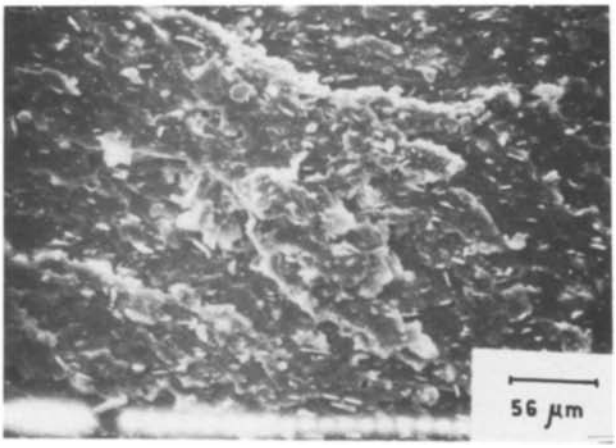

Figure 9 Scanning electron micrograph of the tensile fracture surface of mix C_{S20}, showing enhanced mica–rubber interaction and oriented mica particles.

Westlinning–Wolff (Fig. 4) and Kraüs (Fig. 5) plots. Results of technical properties (Table III) also support this observation.

3.6. Treatment of viscosity data

Table IV shows the observed and calculated values of viscosity data. Observed viscosity values were obtained from minimum rheometric torques (Table III). The viscosity values were calculated according to Einstein [24], Guth–Gold [25] and Guth [26] equations represented by Equations 5, 6 and 7, respectively.

$$\eta = \eta_0 (1 + 2.5\phi) \quad (5)$$

$$\eta = \eta_0 (1 + 2.5\phi + 14.1\phi^2) \quad (6)$$

$$\eta = \eta_0 (1 + 0.67f\phi + 1.62f^2\phi^2) \quad (7)$$

where η_0 is the viscosity of unfilled compound, η the viscosity of filled compound, ϕ the volume fraction of filler, and f the shape factor of filler.

Observed values of viscosity conform well to Equation 5. The effect of polymer–filler interaction on viscosity is taken care of in Equations 6 and 7 through the introduction of second-order terms involving ϕ. Higher theoretical values from these two equations, compared to observed values, signify poor polymer–filler interaction in the present system.

4. Conclusions

Mica marginally increases the moduli and tensile strength of styrene–butadiene rubber (SBR) vulcanizates. However, the increase is more pronounced in the case of tear strength. Mica causes a decrease of volume fraction of rubber (V_r) in benzene-swollen vulcanizates and increases elongation at break. Treatment of mica with a silane coupling agent (A-174) enhances polymer–filler interaction and, consequently, modulus and tensile properties also increase. The increase of heat build-up dynamic set, V_r, and decrease of rebound resilience are also consequences of enhanced wetting of mica by rubber in the presence of a coupling agent. The scanning electron fractograph shows brittle-type failure in the case of SBR gum vulcanizates whereas mica addition makes it ductile-type failure. Orientation of mica along the machine direction is also evident from the scanning electron fractograph. The rheometric viscosity of mica-filled SBR compound fits well to Einstein's hydrodynamic model of particles dispersed in a fluid medium.

References

1. J. LUSIS, MSc thesis, University of Toronto (1970).
2. R. T. WOODHAMS, "Materials Engineering – The next hundred years", Centennial Lecture, Faculty of Applied Science and Engineering, University of Toronto (1974).
3. B. FISA, B. SANCHAGRIN and B. D. FAVIS, *Polym. Compos.* 5(4) (1984) 264.
4. M. XANTHOS, G. C. HAWLEY and J. ANTONACCI, 34th Annual Technical Conference SPE preprints (1976) p. 582.
5. H. P. SCHREIBER, Y. B. TEWARI and M. R. WERTHEIMER, *J. Appl. Polym. Sci.* **20** (1976) 2663.
6. B. FISA and L. A. UTRACKI, *Polym. Compos.* **5**(1) (1984) 36.
7. K. OKUNO and R. T. WOODHAMS, *J. Polym. Engng Sci.* **15**(4) (1975) 308.
8. M. R. WERTHEIMER, L. PAQUIN, H. P. SCHREIBER and S. A. BOGGS, *IEEE Trans Elec. Insul.* **EI-12** (April) (1972) 2.
9. M. R. WERTHEIMER, L. PAQUIN and H. P. SCHREIBER, *J. Appl. Polym. Sci.* **20** (1976) 2675.
10. M. NISHIHARA and J. IMAI, *Fragrance J.* **12**(2) (1984) 114.
11. A. GARTON, *Polym. Compos.* **3**(4) (1982) 189.
12. B. D. FAVIS, L. P. BLANCHAR, J. LEONARD and R. E. PRUD'HOMME, *ibid.* **5**(1) (1984) 11.

TABLE IV Comparison of observed rheometric viscosity with that of calculated values (viscosities are in relative units)

	Mix no.									
	C_0	C_{10}	C_{20}	C_{30}	C_{40}	C_{S0}	S_{10}	S_{20}	S_{30}	S_{40}
Observed	10.5	11.2	12.0	12.8	13.6	11.0	11.5	12.0	12.7	13.5
Einstein equation	–	11.3	12.0	12.8	13.4	–	11.8	12.6	13.4	14.0
Guth–Gold equation	–	11.4	12.6	13.9	15.2	–	12.0	13.2	14.6	15.9
Guth equation	–	11.3	12.3	13.5	14.6	–	11.8	12.9	14.1	15.3

13. Union Carbide Corporation, "Organic-functional silane – A profile", Technical Brochure (1981).
14. S. F. TAUSZ and C. E. CHAFFEY, *J. Appl. Polym. Sci.* **27** (1982) 4493.
15. R. J. ELDRED, *Rubber World* **188**(6) (1983) 26.
16. J. A. WILLIAM, US Natl. Tech. Inform, Service, AD Rep., 750, (1972) 595.
17. B. ELLIS and G. N. WELDING, *Soc. Chem. Ind. London* (1964) p. 46.
18. D. S. CAMPBELL, *J. Appl. Polym. Sci.* **13** (1969) 1201.
19. P. K. PAL and S. K. DE, *Rubber Chem. Technol.* **55** (1982) 1370.
20. H. WESTLINNING and S. WOLFF, *Kautsch. Gummi Kunstst.* **19** (1966) 470.
21. G. KRAÜS, *J. Appl. Polym. Sci.* **7** (1963) 861.
22. *Idem, Rubber Chem. Technol.* **38** (1965) 1070.
23. T. M. MALIK and R. E. PRUD'HOMME, *Polym. Compos.* 7(5) (1986) 315.
24. A. EINSTEIN, *Amer. Phys.* **19** (1906) 289.
25. E. GUTH and O. GOLD, *Phys. Rev.* **53** (1938) 322.
26. E. GUTH, *J. Appl. Phys.* **16** (1945) 20.

Received 23 February
and accepted 15 May 1987